Journal of Inflammation Research

Dovepress
open access to scientific and medical research

Open Access Full Text Article

ORIGINAL RESEARCH

Correlations Between Inflammatory Cell Infiltration and Relative Density and the Boundary Manifestation of Pulmonary Non-Neoplastic Ground Glass Nodules

Xiang-Ling Liu*, Fa-Jin Lv*, Bin-Jie Fu, Rui-Yu Lin, Wang-Jia Li, Zhi-Gang Chu

Department of Radiology, The First Affiliated Hospital of Chongqing Medical University, Chongqing, People's Republic of China

*These authors contributed equally to this work

Correspondence: Zhi-Gang Chu, Department of Radiology, The First Affiliated Hospital of Chongqing Medical University, 1# Youyi Road, Yuanjiagang, Yuzhong District, Chongqing, 400016, People's Republic of China, Tel +86 18723032809, Fax +86 23 68811487, Email chuzg0815@163.com

Purpose: To investigate the influence factors for the various boundary manifestations of pulmonary non-neoplastic ground glass nodules (GGNs) on computed tomography (CT).

Materials and Methods: From January 2015 to March 2022, a total of 280 patients with 318 non-neoplastic GGNs were enrolled. The correlations between degree of inflammatory cell infiltration and relative density (ΔCT) and the boundary manifestations of lesions were evaluated, respectively.

Results: Nongranulomatous nodules (283, 89.0%) with fibrous tissue proliferation and/or inflammatory cells as the predominant pathological findings were the most common non-neoplastic GGNs, followed by granulomatous nodules (28, 8.8%). Among nongranulomatous GGNs, cases with more and less/no inflammatory cells were 15 (10.9%) and 122 (89.1%) in 137 well-defined ones with smooth margin, 16 (24.6%) and 49 (75.4%) in 65 well-defined ones with coarse margin, 43 (91.5%) and 4 (8.5%) in 47 ill-defined ones with higher ΔCT (>151HU), and 4 (11.8%) and 30 (88.2%) in 34 ill-defined ones with lower ΔCT (< 151HU). The proportion of cases with more inflammatory cells in well-defined nodules was similar to that in ill-defined ones with lower ΔCT ($P = 0.587$) but significantly lower than that in ill-defined ones with higher ΔCT ($P < 0.001$). Among the granulomatous nodules, ill-defined cases with higher ΔCT (16, 57.1%) were the most common, and they (7/8, 87.5%) frequently had changes during short-term follow-up.

Conclusion: Nongranulomatous nodules are the most common non-neoplastic GGNs, their diverse boundary manifestations closely correlate with degree of inflammatory cell infiltration and density difference.

Keywords: tomography, X-ray computed, solitary pulmonary nodule, pathology

Introduction

With the increased availability of multi-detector computed tomography (CT) and the advent of low-dose CT screening for lung cancer, an increasing number of pulmonary ground glass nodules (GGNs) have been detected.[1–3] Pathologically, GGNs can be caused by various benign disorders, such as inflammation, edema, fibrosis and hemorrhage, or neoplastic lesions including atypical adenomatous hyperplasia (AAH), adenocarcinoma in situ (AIS), minimally invasive adenocarcinoma (MIA) and invasive adenocarcinoma (IAC).[4,5] Clinically, the treatments for the neoplastic and non-neoplastic GGNs are significantly different.[6] Consequently, it is necessary to distinguish them to facilitate clinical decision-making.

Previous studies have been focusing on investigating the differences in CT features between neoplastic and non-neoplastic GGNs and found that size, shape, boundary, internal solid component, lobulation, spiculation, vessel convergence sign, vacuole sign, air bronchogram, and pleural indentation sign were indicators for differentiating them.[6–8] Specifically, GGNs with solid component (part-solid nodule, PSN), well-defined boundary, vascular

Received: 6 December 2022
Accepted: 24 February 2023
Published: 15 March 2023

convergence sign, larger diameter, lobulation, spiculation, air cavity density, or pleural traction were highly suggestive of neoplastic lesions, while those with irregular shape or ill-defined boundary were considered to be benign ones.[9,10] Although these morphological indicators for differentiating neoplastic and non-neoplastic GGNs were not completely consistent in different studies, it is generally believed that whether the boundary is clear or not is of great value for differentiation.[4,10,11]

Compared with neoplastic GGNs, ill-defined boundary was more frequent in non-neoplastic ones.[10,12] However, a considerable non-neoplastic GGNs can also be well-defined, which indicates the diversity of their boundary manifestation. For the well-defined GGNs, their differential diagnosis is more difficult, and thus follow-up may provide some additional information,[13] while its frequency and duration may be different for the neoplastic and non-neoplastic ones. Currently, there is no yet guidance on this matter. Therefore, understanding the basis for the diverse boundary of non-neoplastic GGNs may be helpful for differentiating diagnosis and determining follow-up strategies. To our knowledge, no studies have yet attempted to investigate the factors responsible for the different boundary manifestations of non-neoplastic GGNs on CT.

The transition of the pathological components and density difference in the lesion-lung boundary zone of GGNs may affect the visual illustration of their boundary. We speculate that the boundary manifestation of non-neoplastic GGNs may be related to their pathological composition and density. Therefore, this study focuses on investigating the correlations between the boundary of non-neoplastic GGNs and their pathological composition and density in order to reveal the basis for the various boundary manifestations. These findings may help to improve the understanding of GGNs and direct further follow-up.

Materials and Methods

This retrospective study was approved by the ethics committee of The First Affiliated Hospital of Chongqing Medical University, and the requirement for informed consent was waived because of the retrospective nature of this study.

Patients

A retrospective data collection of patients with GGNs undergoing CT examinations in our hospital from January 2015 to March 2022 was performed. Cases that met the following conditions were included in this study: (a) nodules were manifested as GGNs on the lung window; (b) GGNs were surgically resected and confirmed as non-neoplastic lesions by pathological examination; and (c) time interval between CT examination and operation was less than 1 weeks. Patients with the following conditions were excluded from the study: (a) no thin-section CT images with a thickness of ≤1 mm; (b) image artifacts that affect the image analysis; and (c) incomplete clinical or pathological data. Finally, a total of 280 patients with 318 GGNs were enrolled in our study.

CT Examinations

The chest CT scans were performed using SOMATOM Perspective (Siemens Healthineers, Erlangen, Germany), and Discovery CT750 HD (GE Healthcare, Milwaukee, WI, USA), and SOMATOM Definition Flash (Siemens Healthineers, Erlangen, Germany) CT scanner. All patients were placed in a supine position with raised upper limbs and were asked to hold their breath after deep inspiration for better exposure. The scan range was from the entrance of the thorax to the costophrenic angle. The scanning parameters were as follows: tube voltage, 110–120 kVp; tube current, 80–250 mAs (reference mAs, using automatic tube current modulation technology); scanning slice thickness, 5 mm; reconstruction slice thickness and interval, 0.625 or 1 mm; matrix: 512 × 512; rotation time, 0.5 s. All images were reconstructed using an iterative reconstruction, and a standard algorithm (GE CT scanners) or medium-sharp algorithm (Siemens CT scanners) was adopted.

Image Analysis

The CT data were analyzed on a PACS workstation (Carestream Vue PACS) with lung window settings (window level, –600 HU; window width: 1500 HU). Two experienced radiologists specializing in chest imaging (Chu with 15 years of experience and Lv with 28 years of experience), who were blinded to the clinical data and histological diagnosis of the

GGNs, independently assessed the CT scans. In case of disagreement, a consensus was reached after a joint discussion and/or consultation with a third senior radiologist.

GGNs were evaluated in the following aspects: (a) size (the average of the longest diameter and the perpendicular diameter on axial images), (b) shape (round, oval, or irregular), (c) location (upper, middle, or inferior lobe), (d) uniformity of density (homogeneous or heterogeneous), (e) CT pattern (pure GGN [pGGN] and PSN), (f) mean CT attenuation, (g) nodule-lung interface (well-defined or ill-defined), (h) margin (smooth, coarse), and (i) other morphological features (lobulation sign, spiculation sign, vacuole sign, pleural indentation, air bronchogram, and containing solid components). Mean CT attenuation (in Hounsfield unit) was measured by placing three to five regions of interest within the ground glass components covering two-thirds of the largest area in GGN and peripheral normal lung tissue while avoiding vessels and bronchioles. The density difference (ΔCT) between the ground glass component in nodules and peripheral normal lung tissue was calculated.

Pathological Analysis

In this study, the rare lesions were not analyzed due to lack of representation. Pathologically, the common GGNs in this study were divided into granulomatous and nongranulomatous lesions. The pathological findings of nongranulomatous nodules included fibrous tissue proliferation and/or inflammatory cells infiltration, fibroblast and myofibroblast hyperplasia, and hyaline degeneration. Pathologically, inflammatory cells infiltration is defined as inflammatory cells, such as neutrophils, eosinophils, lymphocytes, plasmacytes, macrophages, or mast cells, locally or diffusely distributed in lesions. Based on the degree of inflammatory cell infiltration, nongranulomatous nodules were classified into three groups in this study: (1) lesions with more inflammatory cells: multifocal inflammatory cells with a predominance of lymphocytes were detected in nodules; (2) lesions with less inflammatory cells: a few scattered inflammatory cells with a predominance of lymphocytes were detected in nodules; (3) lesions without inflammatory cells infiltration: no significant inflammatory cells were detected in nodules.

Statistical Analysis

All statistical analysis was performed by using SPSS (version 26.0, IBM, NY, USA). Continuous data were expressed as mean ± standard deviation, while categorical variables were expressed as numbers and percentages. For the nongranulomatous and granulomatous nodules, difference in nodule size was evaluated using the Kruskal–Wallis test, and differences in nodule location, CT pattern, and morphological features were analyzed using the Pearson chi-square test or Fisher exact test. Proportions of cases with different degree of inflammatory cell infiltration in nongranulomatous nodules with different boundary manifestations were also analyzed using the Pearson chi-square test. Receiver operating characteristic (ROC) curve analysis was calculated to evaluate the value of ΔCT in predicting the results of subjective assessment for the nodules with higher and lower density. The Youden index was used to determine the optimal cutoff value of Δ CT. A P-value less than 0.05 indicates that the difference was statistically significant.

Results

Clinical Findings

Table 1 summarizes the clinical characteristics of patients. Among the 280 patients, 75 (26.8%) were smokers, 59 (21.1%) had symptoms, 53 (16.7%) had concomitant basic diseases, and 26 (9.3%) had a family history of lung cancer.

Pathological Findings and CT Features of GGNs

Among the 318 GGNs, nongranulomatous lesions (283, 89.0%) with fibrous tissue proliferation and/or inflammatory cells as the predominant pathological findings were the most common, followed by granulomatous lesions (28, 8.8%) (6 cryptococcal infection, 5 tuberculosis infection, and 17 uncertain granulomas), and other rare lesions (7, 2.2%) (4 smooth muscle/spindle cell hyperplasia, 1 hemangioma, 1 hemorrhage, and 1 focal fine bronchialization). The CT features of GGNs are summarized in Table 2. They mainly located in the upper lobes (58.2%), and relatively more lesions were regular (74.8%) and well-defined (68.2%).

Table 1 Patients' Clinical Characteristics

Characteristics	Value
Gender (male / female)	141 (50.4) / 139 (49.6)
Age (years)	53.3 ± 10.9 (24–79)
Smokers	75 (26.8)
Symptoms	59 (21.1)
Fever	2 (3.4)
Cough	47 (79.7)
Sputum	18 (30.5)
Chest pain	12 (20.3)
Phlegm with blood	3 (5.1)
Night sweat	1 (1.7)
Concomitant basic diseases	67 (23.9)
Diabetes	27 (40.3)
Chronic kidney disease	6 (9.0)
Cardiac disease	6 (9.0)
Cerebral infarction	2 (3.0)
Hypothyroidism	4 (6.0)
Hepatic insufficiency	12 (17.9)
Asthma	4 (6.0)
Malignant tumors	14 (20.9)
Family history of lung cancer	26 (9.3)

Notes: Data are presented as n (%), means ± SD or median (range).
Abbreviation: SD, standard deviation.

Table 2 CT Features of Non-Neoplastic GGNs

Characteristics	Nongranulomatous nodules (n = 283)	Granulomatous nodules (n = 28)	*P*-value
Location			0.104[&]
Right Upper lobe	109 (38.5)	5 (17.9)	
Right middle lobe	20 (7.1)	4 (14.3)	
Right lower lobe	52 (18.4)	9 (32.1)	
Left upper lobe	63 (22.2)	5 (17.9)	
Left lower lobe	39 (13.8)	5 (17.9)	
CT pattern			0.001[&]
Pure GGN	154 (54.4)	6 (21.4)	
Mixed GGN	129 (45.6)	22 (78.6)	
Size (mm)	9.7 ± 4.6	13.4 ± 5.6	< 0.001[§]
Shape			0.062[&]
Round/ oval	217 (76.7)	17 (60.7)	
Irregular	66 (23.3)	11 (39.3)	
Boundary			< 0.001[&]
Well-defined	202 (71.4)	9 (32.1)	0.478*
Smooth margin	137 (67.8)	5 (55.6)	
Coarse margin	65 (32.2)	4 (44.4)	
Ill-defined	81 (28.6)	19 (67.9)	
Spiculation	0 (0.0)	1 (3.6)	0.090*
Lobulation	46 (16.3)	1 (3.6)	0.095*
Vacuole	16 (5.7)	0 (0.0)	0.378*
Air bronchogram	22 (7.8)	1 (3.6)	0.707*
Pleural indentation	28 (9.9)	6 (21.4)	0.102*

Notes: Data are presented as n (%), means ± SD or median. [&]Calculated with the Pearson χ^2 test; *Calculated with the Fisher exact test; [§]Kruskal–Wallis test.
Abbreviations: GGN, ground-glass nodule; SD, standard deviation.

Correlations Between Boundary Manifestations and Pathological Composition and Density of GGNs

In view of the high incidence of above-mentioned nongranulomatous nodules and complexity of the pathological components in granulomatous nodules, only the correlations between boundary manifestations of nongranulomatous nodules and their pathological composition and density were further evaluated.

Among the 283 nongranulomatous GGNs, 202 (71.4%) were well-defined and 81 (28.6%) were ill-defined. Pathologically, among the 202 well-defined nodules, cases with more and less/no inflammatory cells were 31 (15.4%) and 171 (84.6%) in the total, 15 (10.9%) and 122 (89.1%) in the 137 ones with smooth margin (Figure 1a and a'), and 16 (24.6%) and 49 (75.4%) in the 65 ones with coarse margin (Figure 1b and b'). Cases with less/no inflammatory cells were predominant in well-defined GGNs, whereas there were more nodules with more inflammatory cells in lesions with coarse margin (Figure 1c and c') than in those with smooth margin (P = 0.012).

For the ill-defined nongranulomatous GGNs, they were subjectively divided into two groups (lesions with higher density and lesions with lower density) based on whether their density was close to that of peripheral normal lung tissue. ROC curve analysis revealed that the threshold value of ΔCT for distinguishing GGNs with higher and lower density was 151 HU (area under the curve ≥0.999, 95% CI: 0.996–1.000, sensitivity and specificity: 97.00% and 100%, P < 0.001). Based on the ΔCT, there were 47 (58.0%) and 34 (42.0%) nodules with higher and lower density among the 81 ill-defined GGNs. Pathologically, cases with more and less/no inflammatory cells were 43 (91.5%) and 4 (8.5%) in the 47 lesions with higher density (Figure 1d and d') and 4 (11.8%) and 30 (88.2%) in the 34 lesions with lower density (Figure 1e and e'). There were more nodules with more inflammatory cells in lesions with higher density than in those with lower density (P < 0.001).

The mean ΔCTs of well-defined nongranulomatous nodules with smooth (255 ± 91HU) or coarse (278 ± 89HU) margin and ill-defined nodules with higher density (246 ± 72HU) were similar (P = 0.122), but they all significantly higher than that of ill-defined nodules with lower density (98 ± 21HU) (P < 0.001). The proportion of cases with more inflammatory cells in the well-defined nodules was similar to that in ill-defined nodules with lower density (P = 0.587) but significantly lower than that in the ill-defined nodules with higher density (p < 0.001).

Among the 28 granulomatous nodules, ill-defined cases with higher density were the most common (16, 57.14%), followed by well-defined cases with smooth (5, 17.86%) or coarse (4, 14.29%) margin, and ill-defined lesions with lower density (3, 10.71%).

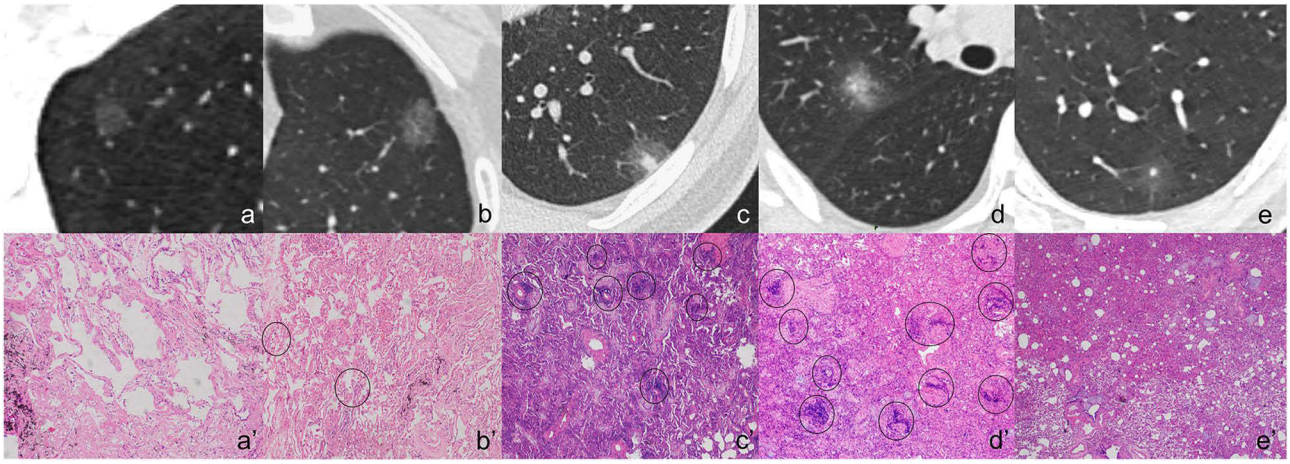

Figure 1 A 52-year-old man with an incidental GGN. (**a**) Axial CT image shows a 6-mm round and well-defined pGGN with smooth margin located in the right upper lobe. (**a'**) Histopathologic analysis reveals fibrous tissue hyperplasia without inflammatory cells. A 76-year-old man with an incidental GGN. (**b**) Axial CT image shows a 17-mm oval and well-defined pGGN with coarse margin located in the left upper lobe. (**b'**) Histopathologic analysis reveals fibrous tissue hyperplasia with less inflammatory cells (black circles). A 24-year-old man with an incidental GGN. (**c**) Axial CT image shows a 17-mm oval and well-defined PSN with coarse margin located in the left lower lobe. (**c'**) Histopathologic analysis reveals fibrous tissue hyperplasia with more inflammatory cells (black circles). A 46-year-old man with cough and expectoration and a smoking history of 20 years. (**d**) His father has lung cancer. Axial CT image shows an 18-mm irregular and ill-defined PSN with higher density (ΔCT=344HU) located in the right upper lobe. (**d'**) Histopathologic analysis reveals fibrous tissue hyperplasia with more inflammatory cells (black circles). A 49-year-old man with backache and a smoking history of 10 years. (**e**) Axial CT image shows a 14-mm oval and ill-defined PSN with lower density (ΔCT = 81HU) located in the left lower lobe. (**e'**) Histopathologic analysis reveals fibrous tissue hyperplasia without inflammatory cells.

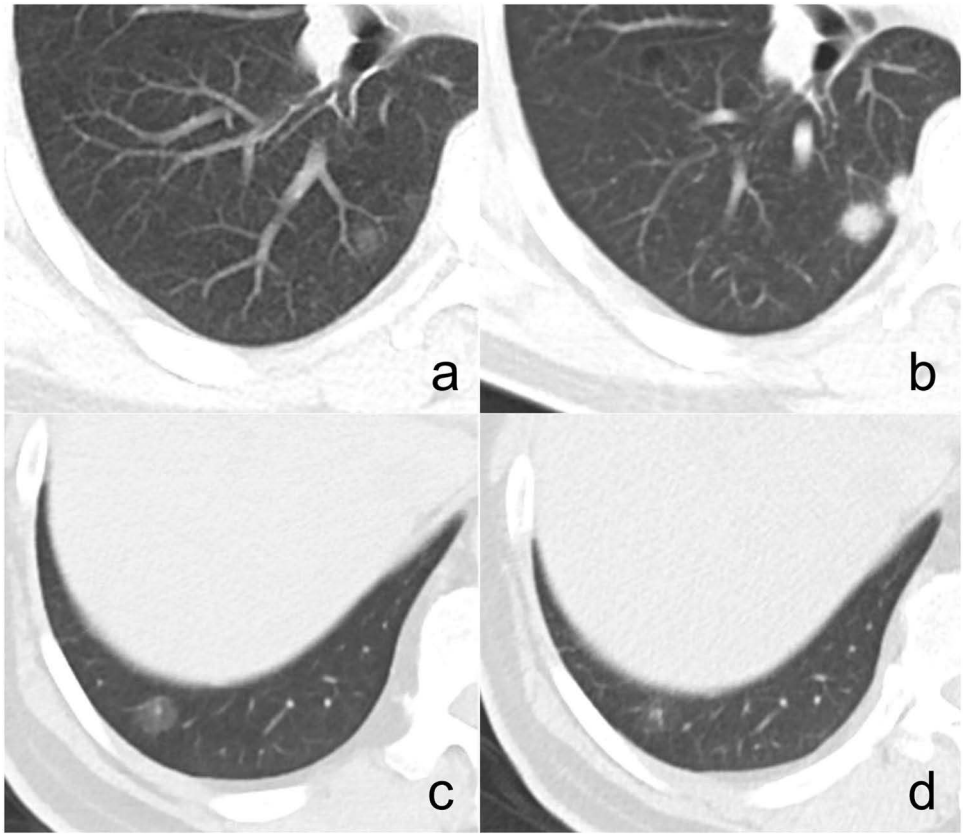

Figure 2 A 57-year-old man with an incidental GGN. (**a**) Axial CT image shows an 8-mm round and ill-defined pGGN with lower density (ΔCT = 105 HU) located in the right lower lobe. (**b**) Follow-up CT scan performed 3 months later shows this nodule increases in size and density and a new solid nodule occurs in the adjacent lung field. Histopathologic analysis reveals granulomatous inflammation caused by cryptococcal infection. A 59-year-old man with diabetes and hepatitis B, and a smoking history of 20 years. (**c**) Axial CT image shows a 12-mm round and well-defined PSN with smooth margin located in the right lower lobe. (**d**) Follow-up CT scan performed one month later shows the nodule decreases in density. Histopathologic analysis reveals granulomatous inflammation.

Follow-Up results

Among the 283 nongranulomatous GGNs, 95 (33.57%) cases were followed up for at least one month (mean, 5.56 ± 11.1 months; range, 1–96 months). There were 57 well-defined nodules with smooth margin (mean follow-up intervals, 4.2 ± 4.4 months; range, 1–19 months), 47 (82.46%) had no significant changes; 21 well-defined nodules with coarse margin (mean follow-up intervals, 9.9 ± 21.4 months; range, 1–96 months), 18 (85.71%) had no significant changes; 12 ill-defined nodules with higher density (mean follow-up intervals, 5.5 ± 6.0 months; range, 1–18 months), 8 (66.67%) had no significant changes, 2 (16.67%) and 2 (16.67%) of them increased and decreased in size and/ or density; 5 ill-defined nodules with lower density (mean follow-up intervals, 3.4 ± 2.1 months; range, 1–6 months), none had significant changes. Among the 28 granulomatous nodules, 8 were followed up for at least one month (2.3 ± 2.0 months, range, 1–7 months), 5 (62.5%) and 2 (25%) of them increased and decreased in size and/or density (Figure 2).

Discussion

In the present study, it was found that a majority of non-neoplastic GGNs were nongranulomatous lesions. Their diverse boundary manifestations on CT images closely correlated with pathological components and density. For the well-defined ones, no matter their margin was smooth or coarse, the main pathological findings were fibrous tissue proliferation with less/no inflammatory cells. In contrast, the ill-defined ones with higher density (ΔCT > 151HU) were mainly consist of fibrous tissue proliferation with more inflammatory cells; however, those with lower density (ΔCT < 151HU) had the similar pathological findings with well-defined GGNs. These findings indicate that the degree of inflammatory cell

infiltration and the density difference between the ground glass component and peripheral normal lung tissue directly affected the boundary display of nongranulomatous GGNs.

Among nongranulomatous GGNs, the well-defined boundary usually indicates the advanced stage of inflammation based on their main pathological findings. However, the proportion of cases with more inflammatory cells in well-defined nodules with coarse margin was higher than that in those with smooth margin. This difference may be related to the fact that these nodules are in different inflammatory processes, and their margin will become smoother with the decrease of inflammatory cell infiltration and proliferation of fibrous tissue.[3,4,14] For the ill-defined GGNs, not only the pathological components but also the density difference (ΔCT) has influence on the display of lesion-lung interface. Regarding those with higher density, the ΔCT is also higher, their blurred boundary may be mainly caused by inflammatory cell infiltration and exudation. However, those with lower density had no significant inflammatory cells, their ill-defined boundary may be mainly relevant to the smaller ΔCT, which makes it difficult to be distinguished visually. Therefore, the density of ground glass component needs to be taken into account when the boundary of GGNs is evaluated. The ill-defined boundary of nodules with lower density may be a "false" CT feature.

Generally, the proportion of ill-defined lesions in non-neoplastic GGNs was significantly higher than that in neoplastic ones, but which varied greatly in different studies.[10–12,15] In the non-neoplastic GGNs that were pathologically confirmed after surgical resection and absorbed during follow-up, this proportion ranged from 43% to 67%.[12,15] In contrast, it ranged from 20% to 61% in studies which only enrolled the pathologically confirmed cases after surgical resection.[10,16] In the present study, only the pathologically confirmed GGNs were enrolled and this proportion was 32.2% among the granulomatous and nongranulomatous lesions, which was lower than that in the samples including absorbed GGNs. This difference may be due to the fact that the well-defined GGNs were more susceptible to be neoplastic than the ill-defined ones, and thus they were more likely to be considered in surgical treatment.[10,17,18] Therefore, it is necessary to pay more attention to differentiate the well-defined GGNs in clinical practice.

In previous studies, it was revealed that the neoplastic GGNs were mainly located in the upper lobe, PSNs had a higher possibility of neoplasm than pGGNs, and lobulation, spiculation, vessel convergence sign, vacuole sign, air bronchogram, and pleural indentation sign were common indicators of neoplastic GGNs.[19–21] However, the present study showed the non-neoplastic GGNs also mainly located in the upper lobes, and PSNs and lesions with some of the above-mentioned signs were also very common in them, which were consistent with the previous findings.[16,22–24] It suggested that there is certain overlap between neoplastic and non-neoplastic GGNs on their distribution and morphological characteristics, which made the differential diagnosis more difficult. For the indeterminate GGNs, follow-up may be a proper strategy, which could provide additional information for diagnosis.[13] The present results may provide some new information for enriching the current follow-up strategy.

For the GGNs, follow-up intervals were usually determined based on their CT findings. From the Fleischner Society 2017, repeated CT at 6–12 months will be considered for pGGN with size ≥6 mm and 3–6 months for PSN with size ≥6 mm and multiple GGNs with any size.[22] In addition, malignant signs were also considered in some studies.[3,25,26] However, no studies have yet taken the boundary of GGNs into account for determining the follow-up intervals. Given the high likelihood of more inflammatory cells, short-term follow-up (3–6 months) should be proper for ill-defined GGNs with higher density because they may have significant changes after inflammation subsides.[27] In contrast, for those ill-defined nodules with lower density and well-defined GGNs (especially those with smooth margin), short-term follow-up may be of little significance owing to they had no or less inflammatory cells but significant fibrous tissue proliferation.[3,28] For these lesions, it should not easily think they are malignant even if they do not give any changes during long-term follow-up. In this study, the changes of some lesions during follow-up partly verified our infer. Thus, the boundary and density of GGNs should also be considered in determining follow-up intervals.

In the present study, the second most common non-neoplastic GGNs were granulomatous lesions, which had the similar CT manifestations of nongranulomatous lesions. Most of them were ill-defined and had higher density, which indicated they were in an active phase of infection. Although the ill-defined boundary supported the diagnosis of benign lesions for the granulomatous nodules, they can also be well-defined, which made it is difficult for diagnosis. The follow-up information of granulomatous GGNs suggested that those lesions usually changed rapidly in short-term, which was different from nongranulomatous lesions. Therefore, if a GGN changed rapidly, especially increasing in size and/or

density, it is more likely to be granulomatous lesion. Further examinations for fungal or tuberculous infection may provide more information for diagnosis.

There are four limitations in the present study. First, the nongranulomatous and granulomatous GGNs were respectively studied in this study due to their pathological differences. However, they cannot be well differentiated by CT in clinical practice. Thus, some findings from nongranulomatous nodules may be inconsistent with those of granulomatous lesions. Second, the evaluation for the degree of inflammatory cell infiltration in lesions was subjective. Third, the sample size with routine follow-up information was small due to the retrospective nature of this study. Thus, the value of current results in directing follow-up need to be further verified in clinical practice. Fourth, the etiology of some granulomatous GGNs were unknown.

Conclusion

In conclusion, most of the non-neoplastic GGNs are nongranulomatous lesions, their boundary manifestations are related to the pathological compositions and density. More inflammatory cells and lower relative density mainly contribute to the ill-defined boundary of nodules. For well-defined GGNs with coarse margin and ill-defined GGNs with higher density, short-term follow-up may be more meaningful in view of the higher probability of containing more inflammatory cells. Granulomatous GGNs are relatively rare, but they frequently have changes during short-term follow-up. Better understanding of these CT features and corresponding pathological basis of common non-neoplastic GGNs could contribute to the accurate diagnosis, reduction in the number of unnecessary operations, and advancements in determining an optimal management strategy.

Ethics Statement

The study was conducted in accordance with the Declaration of Helsinki, and the protocol was approved by the Ethics Committee of the First Affiliated Hospital of Chongqing Medical University (No. 2019-062), which absolved the need for written informed consent because of the retrospective study. All personal identification data were anonymized and de-identified before analysis.

Consent for Publication

All of the images, tables and recordings can be published.

Funding

This work was supported by the Joint Project of Chongqing Science and Technology Commission and Chongqing Public Health Commission (2022MSXM050) and the Senior Medical Talents Program of Chongqing for Young and Middle-aged from Chongqing Health Commission (Receptor: Zhi-Gang Chu).

Disclosure

All authors declare no conflicts of interest for this work.

References

1. Kim TJ, Goo JM, Lee KW, Park CM, Lee HJ. Clinical, pathological and thin-section CT features of persistent multiple ground-glass opacity nodules: comparison with solitary ground-glass opacity nodule. *Lung Cancer*. 2009;64(2):171–178. doi:10.1016/j.lungcan.2008.08.002
2. Chu ZG, Li WJ, Fu BJ, Lv FJ. CT Characteristics for predicting invasiveness in pulmonary pure ground-glass nodules. *AJR Am J Roentgenol*. 2020;215(2):351–358. doi:10.2214/AJR.19.22381
3. Qin Y, Xu Y, Ma D, et al. Clinical characteristics of resected solitary ground-glass opacities: comparison between benign and malignant nodules. *Thorac Cancer*. 2020;11(10):2767–2774. doi:10.1111/1759-7714.13575
4. Fan L, Liu SY, Li QC, Yu H, Xiao XS. Multidetector CT features of pulmonary focal ground-glass opacity: differences between benign and malignant. *Br J Radiol*. 2012;85(1015):897–904. doi:10.1259/bjr/33150223
5. Kim HY, Shim YM, Lee KS, Han J, Yi CA, Kim YK. Persistent pulmonary nodular ground-glass opacity at thin-section CT: histopathologic comparisons. *Radiology*. 2007;245(1):267–275. doi:10.1148/radiol.2451061682
6. Hu H, Wang Q, Tang H, Xiong L, Lin Q. Multi-slice computed tomography characteristics of solitary pulmonary ground-glass nodules: differences between malignant and benign. *Thorac Cancer*. 2016;7(1):80–87. doi:10.1111/1759-7714.12280

7. Gao F, Li M, Ge X, et al. Multi-detector spiral CT study of the relationships between pulmonary ground-glass nodules and blood vessels. *Eur Radiol*. 2013;23(12):3271–3277. doi:10.1007/s00330-013-2954-3
8. Yoon HE, Fukuhara K, Michiura T, et al. Pulmonary nodules 10 mm or less in diameter with ground-glass opacity component detected by high-resolution computed tomography have a high possibility of malignancy. *Jpn J Thorac Cardiovasc Surg*. 2005;53(1):22–28. doi:10.1007/s11748-005-1004-8
9. Felix L, Serra-Tosio G, Lantuejoul S, et al. CT characteristics of resolving ground-glass opacities in a lung cancer screening programme. *Eur J Radiol*. 2011;77(3):410–416. doi:10.1016/j.ejrad.2009.09.008
10. He XQ, Li X, Wu Y, et al. Differential diagnosis of nonabsorbable inflammatory and malignant subsolid nodules with a solid component ≤5 mm. *J Inflamm Res*. 2022;15:1785–1796. doi:10.2147/JIR.S355848
11. Hsu WC, Huang PC, Pan KT, et al. Predictors of invasive adenocarcinomas among pure ground-glass nodules less than 2 cm in diameter. *Cancers*. 2021;13(16):3945. doi:10.3390/cancers13163945
12. Fu BJ, Lv FJ, Li WJ, Lin RY, Zheng YN, Chu ZG. Significance of intra-nodular vessel sign in differentiating benign and malignant pulmonary ground-glass nodules. *Insights Imaging*. 2021;12(1):65. doi:10.1186/s13244-021-01012-7
13. Hammer MM, Palazzo LL, Eckel AL, Barbosa EM, Kong CY. A decision analysis of follow-up and treatment algorithms for nonsolid pulmonary nodules. *Radiology*. 2019;290(2):506–513. doi:10.1148/radiol.2018180867
14. Yang PS, Lee KS, Han J, Kim EA, Kim TS, Choo IW. Focal organizing pneumonia: CT and pathologic findings. *J Korean Med Sci*. 2001;16(5):573–578. doi:10.3346/jkms.2001.16.5.573
15. Li WJ, Lv FJ, Tan YW, Fu BJ, Chu ZG. Pulmonary benign ground-glass nodules: CT features and pathological findings. *Int J Gen Med*. 2021;14:581–590. doi:10.2147/IJGM.S298517
16. Mei X, Wang R, Yang W, et al. Predicting malignancy of pulmonary ground-glass nodules and their invasiveness by random forest. *J Thorac Dis*. 2018;10(1):458–463. doi:10.21037/jtd.2018.01.88
17. Yang W, Sun Y, Fang W, et al. High-resolution computed tomography features distinguishing benign and malignant lesions manifesting as persistent solitary subsolid nodules. *Clin Lung Cancer*. 2018;19(1):e75–e83. doi:10.1016/j.cllc.2017.05.023
18. Nambu A, Araki T, Taguchi Y, et al. Focal area of ground-glass opacity and ground-glass opacity predominance on thin-section CT: discrimination between neoplastic and non-neoplastic lesions. *Clin Radiol*. 2005;60(9):1006–1017. doi:10.1016/j.crad.2005.06.006
19. Watanabe S, Watanabe T, Arai K, Kasai T, Haratake J, Urayama H. Results of wedge resection for focal bronchioloalveolar carcinoma showing pure ground-glass attenuation on computed tomography. *Ann Thorac Surg*. 2002;73(4):1071–1075. doi:10.1016/S0003-4975(01)03623-2
20. Kodama K, Higashiyama M, Yokouchi H, et al. Prognostic value of ground-glass opacity found in small lung adenocarcinoma on high-resolution CT scanning. *Lung Cancer*. 2001;33(1):17–25. doi:10.1016/S0169-5002(01)00185-4
21. Qiu ZX, Cheng Y, Liu D, et al. Clinical, pathological, and radiological characteristics of solitary ground-glass opacity lung nodules on high-resolution computed tomography. *Ther Clin Risk Manag*. 2016;12:1445–1453. doi:10.2147/TCRM.S110363
22. MacMahon H, Naidich DP, Goo JM, et al. Guidelines for management of incidental pulmonary nodules detected on CT images: from the Fleischner society 2017. *Radiology*. 2017;284(1):228–243. doi:10.1148/radiol.2017161659
23. Lindell RM, Hartman TE, Swensen SJ, et al. Five-year lung cancer screening experience: CT appearance, growth rate, location, and histologic features of 61 lung cancers. *Radiology*. 2007;242(2):555–562. doi:10.1148/radiol.2422052090
24. Horeweg N, van der Aalst CM, Thunnissen E, et al. Characteristics of lung cancers detected by computer tomography screening in the randomized Nelson trial. *Am J Respir Crit Care Med*. 2013;187(8):848–854. doi:10.1164/rccm.201209-1651OC
25. Shi Z, Chen C, Jiang S, Jiang G. Uniportal video-assisted thoracic surgery resection of small ground-glass opacities (GGOs) localized with CT-guided placement of microcoils and palpation. *J Thorac Dis*. 2016;8(7):1837–1840. doi:10.21037/jtd.2016.06.12
26. Ley S, Ley-Zaporozhan J. Novelties in imaging in pulmonary fibrosis and nodules. *A Narrative Review Pulmonology*. 2020;26(1):39–44.
27. Godoy MC, Naidich DP. Overview and strategic management of subsolid pulmonary nodules. *J Thorac Imaging*. 2012;27(4):240–248. doi:10.1097/RTI.0b013e31825d515b
28. Park CM, Goo JM, Lee HJ, et al. Focal interstitial fibrosis manifesting as nodular ground-glass opacity: thin-section CT findings. *Eur Radiol*. 2007;17(9):2325–2331. doi:10.1007/s00330-007-0596-z